IEEE Access
Multidisciplinary | Rapid Review | Open Access Journal

Received July 13, 2019, accepted July 22, 2019, date of publication August 1, 2019, date of current version September 3, 2019.

Digital Object Identifier 10.1109/ACCESS.2019.2931995

Optimization of Reconstruction Accuracy of Anomaly Position Based on Stacked Auto-Encoder Neural Networks

HUIQUAN WANG[1,2], NIAN WU[1], YU CAI[1], LINA REN[1], ZHE ZHAO[2], GUANG HAN[1,2], AND JINHAI WANG[1,2]

[1]School of Life Sciences, Tianjin Polytechnic University, Tianjin 300387, China
[2]Tianjin Key Laboratory of Optoelectronic Detection Technology and Systems, Tianjin 300387, China

Corresponding author: Jinhai Wang (tjpubme@126.com)

This work was supported in part by the National Natural Science Foundation of China (Grant No. 61705164 and Grant No. 81901789) and 61 batch of China Post-Doctoral Science Foundation.

ABSTRACT The diffuse optical tomography (DOT) technique which uses the traditional linear iterative algorithm has the problems of slow calculation speed and low reconstruction imaging accuracy in the inverse problem reconstruction, which limits its clinical application and development. This paper proposes an inverse-problem solving technology based on a stacked auto-encoder (SAE) network to improve the reconstruction accuracy of anomaly position, size and absorption coefficient in tissues. The reconstruction accuracy of anomaly position, size and absorption coefficient obtained by the traditional algebraic reconstruction technique (ART) method and the SAE based method are experimentally compared. The experimental results show that the SAE based method achieves the prediction accuracy of anomaly position of 96.25%, thus improving the accuracy and shortening the reconstruction time compared with the traditional ART method. Accordingly, the proposed method provides a better solution to the problem of the inaccurate reconstruction of the position and size of the rapid DOT based positioning of anomalies.

INDEX TERMS Diffuse optical tomography, image reconstruction, stacked auto-encoder network.

I. INTRODUCTION.

The near-infrared spectroscopy for detection of biological tissue components has the advantages of excellent real-time performance, and continuous, non-invasive, and low-cost, characteristics. The diffuse optical tomography (DOT) technique [1] for detection of tissue components and imaging diagnosis of organisms has been widely applied in cerebral hematoma diagnosis [2], brain functional imaging [3], early screening and diagnosis of breast cancer [4], etc. The DOT technique reflects or transmits a signal through a biological tissue using one or more light sources, and acquires boundary data of the tissue using a plurality of detector arrays, thereby reconstructing the optical parameters of a cross-section of biological tissue. The fast and accurate reconstruction of inverse problems in biomedical imaging has been a research hotspot in the field of biomedical imaging [5], [6]. The inverse problem of the traditional DOT is mostly solved by using the algebraic iterative algorithm, but due to its complicated structure, the nonlinear problem [7] of scattering, and high time consumption, the computational complexity of inverse problem reconstruction is increased [8], thus failing to meet the requirements for rapid imaging.

In recent years, due to the rapid development of deep neural networks [9]–[11], they have been widely applied to various fields for feature extraction and classification of complex models. In [12], the neural network approach was adopted to reconstruct the optical parameters of biological tissues to overcome the shortcomings of traditional reconstruction methods such as a long calculation time and limited optical parameter range, providing the advantages of wide adaptability, and high accuracy and stability.

In this paper, we aim to solve the DOT reconstruction problem related to the optical parameters of anomalies and establish an anomaly detection model based on deep neural networks. The Single-Source Multi-Detectors method is used to obtain the light intensity detected by the detector, and implement the feature extraction from the input layer to

The associate editor coordinating the review of this manuscript and approving it for publication was Wen Chen.

the output layer. The SAE algorithm [13] is used to realize the feature extraction and analyze the position and size of anomalies, optimizing the recognition rate. The proposed method for reconstructing the anomaly position using an SAE deep neural network can be used as an effective tool for anomaly detection and rapid evaluation of anomaly position. Also, it can provide a basis for improved methods for tumor detection [14] and early screening of breast cancer [15].

II. SAE NEURAL NETWOR.

The stacked auto-encoder (SAE) depth neural network [16] is an efficient unsupervised feature recognition and deep learning method, which is widely used in various feature extraction and classification problems. With the aim to realize the reconstruction of anomaly position in biological tissue, we use a deep neural network composed of a double hidden layer SAE [17] to solve the inverse problem of the DOT. The neural network includes a number of layers, where the output of the former layer denotes the input data of the next layer. It is layer-by-layer training in the order from front to back, and each hidden layer denotes a higher layer abstraction of the previous layer. The last layer is the softmax classifier. The SAE working principle is shown in Fig. 1.

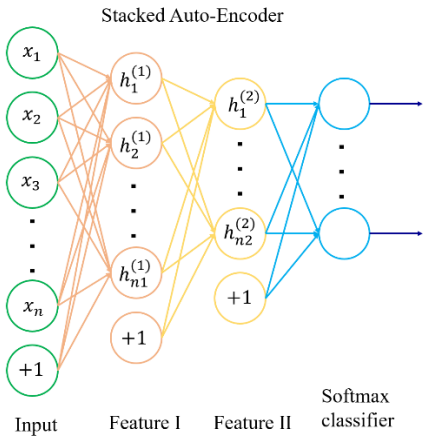

FIGURE 1. The structure of the stacked auto-encoder neural network.

The SAE network denotes a feedback neural network model composed of multiple auto-encoders (AEs). The auto-encoder represents a three-layer neural network consisted of an input layer, a hidden layer, and an output layer. The neurons form the adjacent layers are completely interconnected. The auto-encoder uses the activation function of the first layer of the neural network to extract the features of the input data and forward it to the following hidden layer. In this work, the sigmoid activation function is used, and it is given by:

$$f(x) = \frac{1}{1 + e^{-x}}. \tag{1}$$

The network training process includes two parts: unsupervised pre-training and supervised NN-training, which are presented in Fig. 2(a) and Fig. 2(b), respectively. The pre-training denotes the training process used to adjust the values

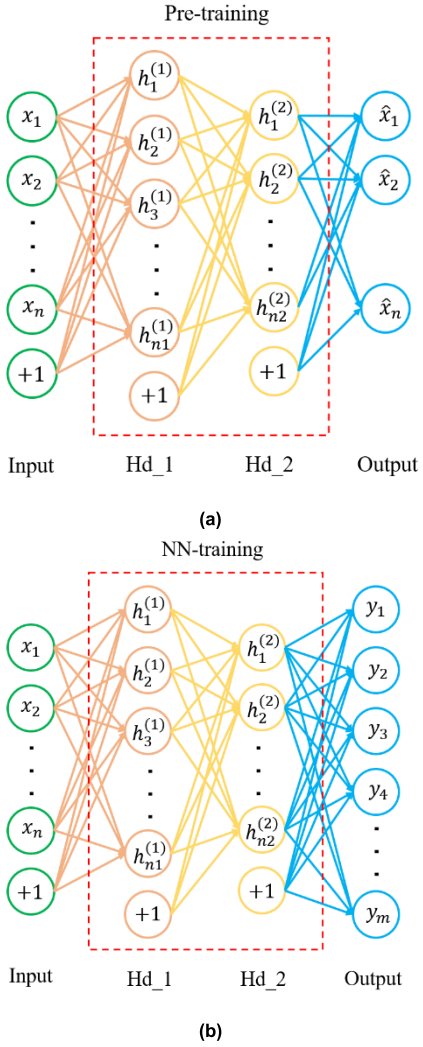

FIGURE 2. The unsupervised pre-training (a) and supervised NN-training (b) of an SAE neural network.

of network weights and biased using unsupervised learning. The original data is used as the input of the SAE network, and the network parameters of the first hidden layer are trained by encoding and decoding. The output of the first AE is used as the input of the next AE, and the weight and deviation of the network layer are trained in the same way. The supervised NN-training is to use the obtained network weights and deviations as initial values into the Back-propagation (BP) neural network for further training using supervised learning. The BP algorithm trains the neural network using the forward conduction and then uses the backpropagation algorithm to fine-tune network parameters to determine the optimal neural network parameters to obtain a network with two hidden layers. The working principle of the model structure used in this study is shown in Fig. 2.

The input of the network model is the intensity value collected by the detector, and the output is the absorption coefficient of the biological tissue. Number of epoch is 49.

Stop criteria is complete the preset 100 iterations. The number of iterations is obtained by tuning the preferences. The network training time on the CPU of the Intel(R) Core(TM) i5-8400 is about 2 hours.

III. DOT SIMULATION AND ANOMALY RECONSTRUCTION

A. DOT SIMULATION MODEL

To realize the image reconstruction of the anomaly position in the biological tissue by using the SAE deep neural network, the Nirfast software was used to obtain training data. Nirfast is an optical imaging software developed by the Dartmouth College Biomedical Engineering team in the United States, which is based on the finite element method that is used to establish a model of the light transmission through the measured object such as biological tissue. A uniform two-dimensional rectangular model with the size of 40 mm × 90 mm was established by Nirfast optical finite element tool. The background optical parameters were $\mu_a = 0.01$ mm^{-1} and $\mu_s' = 1$ mm^{-1}. The Source-Detector position of the model is shown in Fig. 3. The coordinate system was established such that the model endpoint denoted the coordinate system origin. The light source was located at 5 mm from the coordinate system origin. Ten detectors labeled from D1 to D10 were equidistantly distributed starting from 13 mm to 85 mm from the coordinate system origin. The distance between the light source and the first detector was 8 mm, and the distance between adjacent detectors was also set 8 mm to obtain the light intensity measured by 10 detectors.

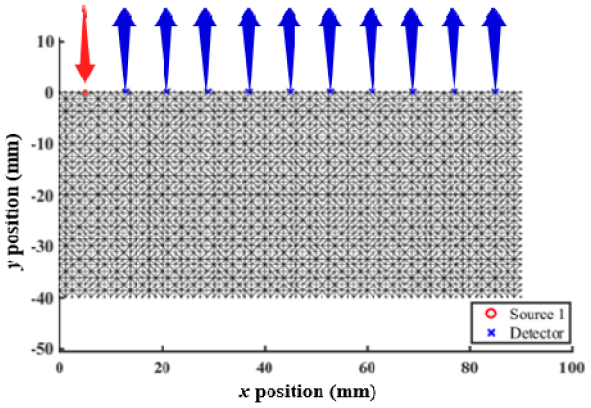

FIGURE 3. Schematic diagram of model splitting results.

The Nirfast optical finite element tool was used to generate the simulation training datasets fast and efficiently. The finite element generated segmentation mesh was converted into a voxel matrix by using the nearest neighbor difference based on the triangulation. The model that is presented in Fig. 3 was divided into 2409 splitting units, and the size of each splitting unit was 1.25 mm. An anomaly was added to the uniform tissue model, and it was moved through the simulation model so that to traverse the entire model, and 430 datasets containing the information about the anomalies at different positions were generated. In the simulation model, the anomaly radius was 10 mm, and its optical parameters were set to $\mu_a = 0.5$ mm^{-1}, $\mu_s' = 1$ mm^{-1}.

B. SAE NEURAL NETWORK MODELING

A two-hidden-layer SAE deep neural network which has four layers in total was adopted. The input data of the SAE neural network was the reflected light intensity detected by multiple detectors in the simulation model, and the output data was the absorption coefficient of each triangle-splitting unit in the simulation model. The SAE neural network had 10 neurons in the input layer, 200 neurons and 60 neurons in the first and second hidden layers, respectively, and 2409 neurons in the output layer.

The training datasets and the prediction datasets were selected before establishing the SAE neural network. The data equalization distribution method was adopted to perform equal distance cross-selection of collected data samples to obtain training datasets and prediction datasets. Namely, since the training and prediction datasets were processed by the method of data equalization distribution selection, the SAE method achieved the prediction accuracy of anomaly position of 96.25%. The dataset samples represented the optical information about the anomaly at different positions, while the method of randomly selecting the data would introduce a large error, and it would be easy to generate an accidental error due to the incomplete selection of the training datasets. Therefore, to realize high learning effect of the SAE neural network when the anomaly was moved through the tissue model, the data equalization distribution method was used to select training datasets and prediction datasets.

IV. RESULTS AND DISCUSSION

A. SAE NEURAL NETWORK RECONSTRUCTION RESULTS

To determine the anomaly position in the tissue using the method based on the SAE deep neural network, the radius of the anomaly was set to 10 mm, and the dataset of 430 samples was used for model training and testing, of which 350 samples constituted the training datasets, and 80 samples constituted the test datasets. As already mentioned, the SAE neural network consisted of four layers having 10, 200, 60, and 2409 neurons, respectively. The number of training iterations was set to 100. The obtained reconstruction results are shown in Fig. 4.

In Fig. 4, on the left side, the actual distribution of the true absorption coefficient μ_a of the tissue model containing the anomaly is presented, and the actual distribution of the predicted absorption coefficient μ_a of the same tissue model predicted by the SAE neural network model is presented on the right side. The prediction accuracy of anomaly position of more than 95% was achieved using the proposed neural network model.

According to the prediction results of five groups of anomalies at different lateral positions and different depths, the SAE neural network can be used to reconstruct the

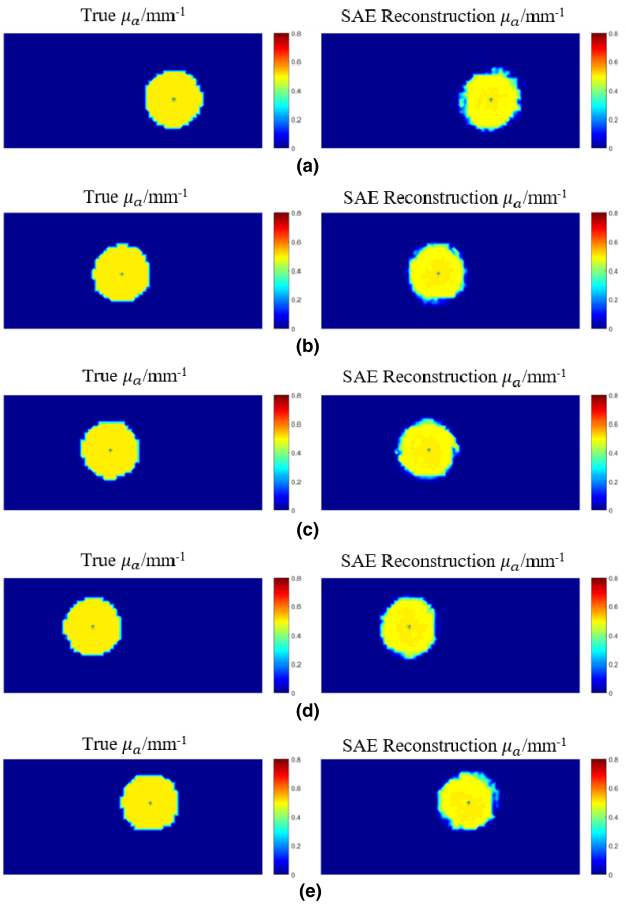

FIGURE 4. The reconstruction results obtained by the proposed SAE neural network.

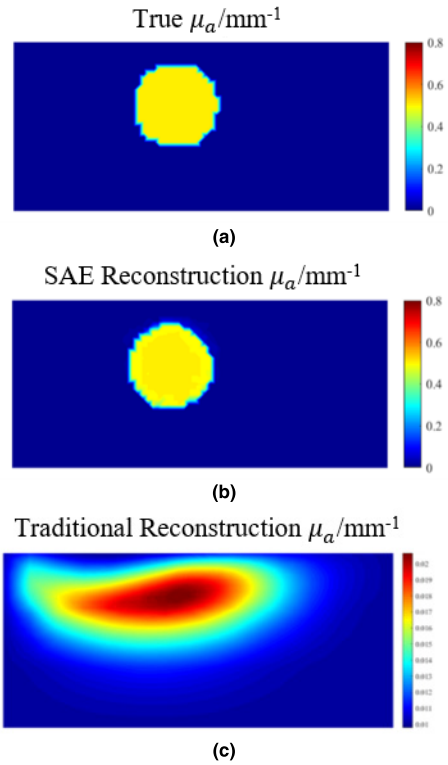

FIGURE 5. Comparison of the traditional ART reconstruction method and the proposed SAE based reconstruction method.

anomaly position and obtain a good recognition rate, that is, the SAE neural network can predict the lateral position of the anomaly and the longitudinal depth of the anomaly.

B. COMPARISON OF SAE NEURAL NETWORK AND ART RECONSTRUCTION

To evaluate the image reconstruction results obtained by the proposed reconstruction method, the obtained results were compared with those of the traditional ART reconstruction. The results for comparison were selected under the same position and parameters in the dataset. The traditional ART reconstruction used the Levenberg-Marquardt algorithm for inverse problem reconstruction. The maximum number of iterations for reconstruction was set to 100. The comparison reconstruction results are shown in Fig. 5.

Fig. 5(a) show the actual distribution of the true absorption coefficient μ_a of the tissue model containing the anomaly. Fig. 5(b) show the actual distribution of the predicted absorption coefficient μ_a of the tissue model predicted by SAE neural network. Fig. 5(c) show the actual distribution of the absorption coefficient μ_a of the tissue model obtained from reconstruction by the traditional ART reconstruction method. Compared with the traditional ART reconstruction method, the SAE neural network achieved higher feature recognition rate for anomaly position reconstruction. The reconstruction results show that the SAE neural network has great advantages in determining the size and position of anomaly and reconstruction of its optical parameters. Thus, the proposed method has better recognition ability than the traditional ART reconstruction method in determining the anomaly position.

In the simulations, the traditional ART reconstruction method was slow due to a large amount of computation. On the other hand, due to the simple structure, the SAE network-based method reduced the computational complexity, shortened the reconstruction time of anomaly position, and realized fast and accurate positioning of the anomaly position.

C. SAE NEURAL NETWORK RECONSTRUCTION RESULTS ANALYSIS

To quantitatively evaluate the SAE neural network regarding the reconstruction accuracy of anomaly position, we compared the actual anomaly central position of 80 predicted data samples with those predicted by the SAE neural network. The actual distance, called the Euclidean distance, was calculated by:

$$\rho = \sqrt{(x_2 - x_1)^2 + (y_2 - y_1)^2}. \tag{2}$$

In (2), ρ represents the Euclidean distance, x_1 and y_1 respectively represent the horizontal and vertical coordinates

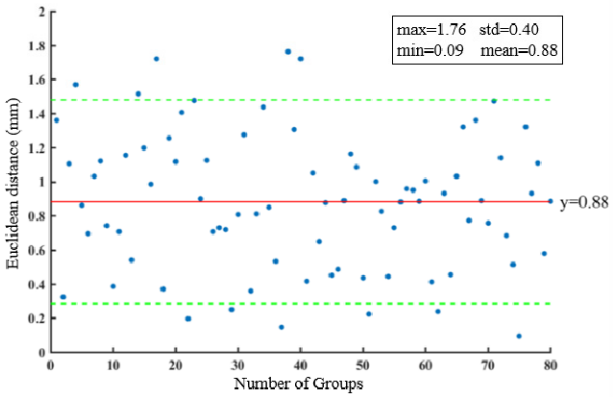

FIGURE 6. The Euclidean distance distribution of 80 samples.

of the actual anomaly center position, and, x_2 and y_2 respectively represent the horizontal and vertical coordinates of the anomaly center position predicted by the SAE neural network. The stability and accuracy of the SAE neural network model were judged by analyzing the Euclidean distance distribution of the real and predicted data. Fig. 6 shows the Euclidean distance distribution of 80 predicted samples. As can be seen in Fig. 6, the SAE prediction results were relatively accurate except in the cases where there were accidental errors such as that of the model splitting unit size. Besides, the maximum, minimum, mean, and standard deviations of the Euclidean distance of the predicted samples were determined. The red line in Fig. 6 represents the average value of the Euclidean distance of the predicted samples, and the green dashed area indicates three times the standard deviation of the Euclidean distance of the predicted samples. As can be seen in Fig. 6, the Euclidean distance of the predicted samples was more than 90% scattered in the green area, and the Euclidean distance of only 5 samples was larger than the upper limit of the green area. The difference between the predicted and real data was within an acceptable range, further confirming the high prediction accuracy of the SAE neural network model.

At the same time, the anomaly center position within the lateral position of 30-60 mm and the longitudinal position of 15-23 mm was compared for real and predicted data. The obtained comparison results in both x and y directions are shown in Fig. 7.

Fig. 7(a) shows the difference between the true and predicted values of different lateral positions in the x-direction. The curve in Fig. 7(a) can be approximated as a straight line with a slope close to 1, the prediction accuracy of the SAE neural network in the x-direction was high. By observing the error of the curve, it can be found that the existing data error is derived from the influence of the anomaly at different depths on the prediction of the lateral position. The error distribution presented in Fig. 7 show that when the anomaly was located in the middle of the detector array, the influence of the depth error was small, and the prediction accuracy of the SAE neural network was high. Fig.7(b) shows the difference between

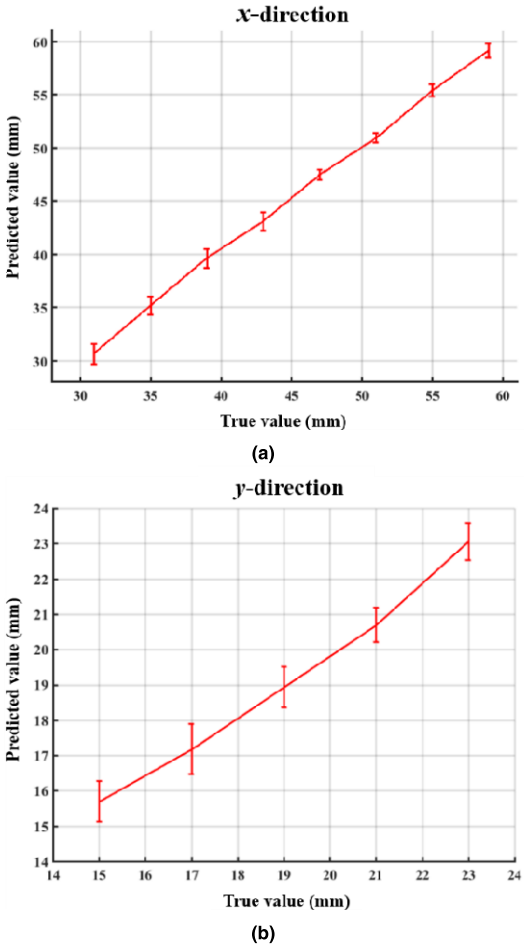

FIGURE 7. Difference between real and predicted values.

the true and predicted values of different longitudinal positions in the y-direction. The curve in Fig. 7(b) can also be approximated as a straight line with a slope close to 0.9, and the error of the predicted values did not exceed 1 mm; the error resulted from the effect of predicting the anomaly depth when the anomalies were at different lateral positions.

Consequently, the difference between the true and predicted values presented in Fig. 7 demonstrates that the proposed SAE neural network based method represents an excellent solution to the problem of inaccurate depth prediction in the reflection DOT.

D. SAE NEURAL NETWORK RECONSTRUCTION RESULTS UNDER NOISE

In order to evaluate the noise immunity of the network used, we added noise to the dataset samples. Fig. 8 shows the network reconstruction result after adding different noises. Fig. 8 (a)-(d) were reconstruction results after adding 20 dB, 40 dB, 60 dB and 80 dB noise respectively.

Fig. 8 shows the network we used after adding noise can still reconstruct the location and size of the anomaly. For this, we also compared the anomaly center positions of

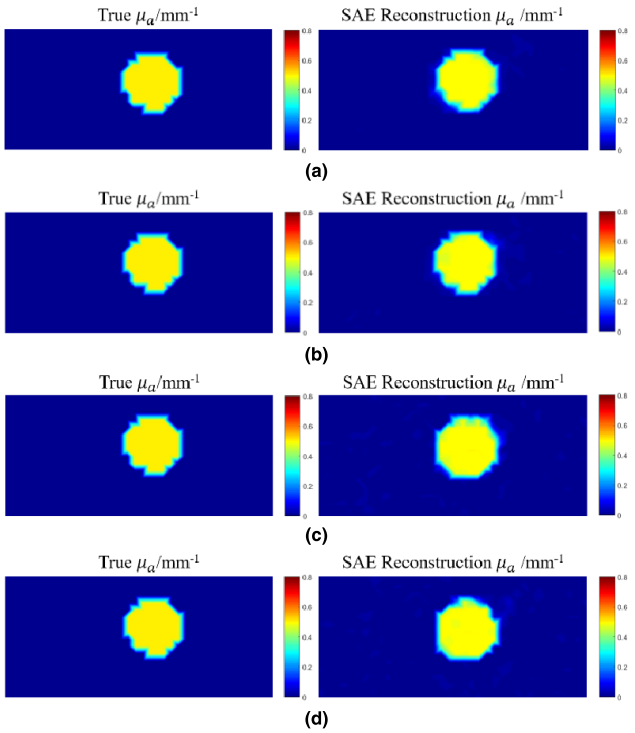

FIGURE 8. Network reconstruction result under different noises.

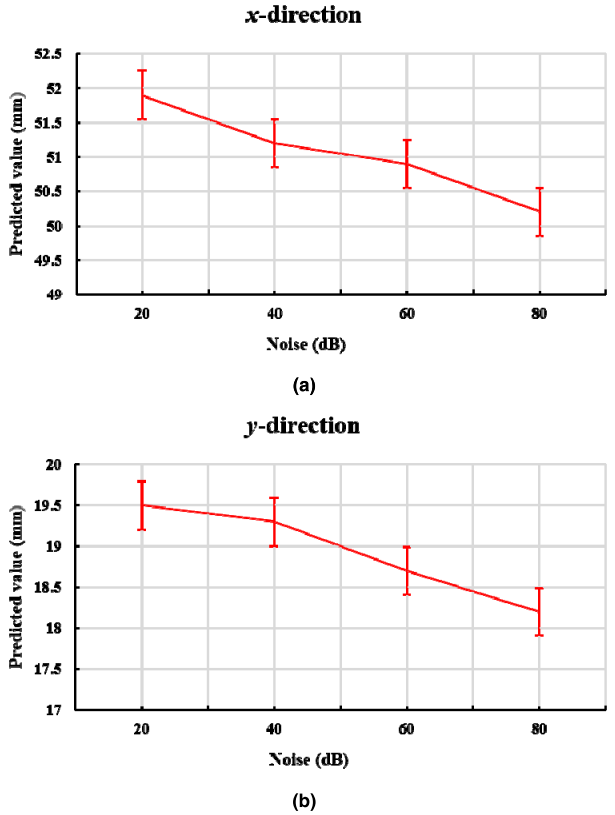

FIGURE 9. The center position of anomaly under different noises.

the lateral and longitudinal positions of the predicted data under different noises. The comparison results obtained in the x and y directions are shown in Fig. 9.

Fig. 9(a) shows the center position of the anomaly in the x-direction under different noises. Fig. 9(b) shows the center position of the anomaly in the y-direction under different noises. The center position of the true anomaly in the x-direction is 50 mm, and the center position of the real anomaly in the y-direction is 18 mm. The position and size error of the anomaly reconstructed by the network is not more than 2 mm, which proves the good noise resistance of the network.

V. CONCLUSION

This study proposes a reconstruction method for anomaly position based on the SAE neural network. The SAE neural network intended for rapid detection of anomaly position is constructed by using the Single-Source Multi-Detectors distribution of light intensity collected on the biological tissues surface. The proposed method is evaluated by simulations, and the obtained results show that the SAE neural network exhibits great advantages regarding the accuracy and stability of anomaly position reconstruction compared with the traditional linear iterative algorithm. Due to the simple structure and short reconstruction time, the proposed method can be used as an effective tool for rapid determination of anomaly position in biological tissues in the clinical tasks.

REFERENCES

[1] K. Prieto and O. Dorn, "Sparsity and level set regularization for diffuse optical tomography using a transport model in 2D," *Inverse Problems*, vol. 33, no. 1, Nov. 2017, Art. no. 014001.

[2] X. Dai, T. Zhang, H. Yang, J. Tang, P. R. Carney, and H. Jiang, "Fast noninvasive functional diffuse optical tomography for brain imaging," *J. Biophoton.*, vol. 11, no. 3, Sep. 2018, Art. no. e201600267.

[3] A. T. Eggebrecht, S. L. Ferradal, A. Robichaux-Viehoever, M. S. Hassanpour, H. Dehghani, A. Z. Snyder, T. Hershey, and J. P. Culver, "Mapping distributed brain function and networks with diffuse optical tomography," *Nature Photon.*, vol. 8, no. 6, pp. 448–454, May 2014.

[4] J. E. Gunther, E. A. Lim, H. K. Kim, M. Flexman, M. Altoé, J. A. Campbell, H. Hibshoosh, K. D. Crew, K. Kalinsky, D. L. Hershman, and A. H. Hielscher, "Dynamic diffuse optical tomography for monitoring neoadjuvant chemotherapy in patients with breast cancer," *Radiology*, vol. 287, no. 3, pp. 778–786, Feb. 2018.

[5] J. C. Bore, W. M. A. Ayedh, P. Li, D. Yao, and P. Xu, "Sparse autoregressive modeling via the least absolute LP-norm penalized solution," *IEEE Access*, vol. 7, pp. 40959–40968, Jul. 2019.

[6] J. C. Bore, C. Yi, P. Li, F. Li, D. J. Harmah, Y. Si, D. Guo, D. Yao, F. Wan, and P. Xu, "Sparse EEG source localization using LAPPS: Least absolute LP (0<p<1) penalized solution," *IEEE Trans. Biomed. Eng.*, vol. 66, no. 7, pp. 1927–1939, Jul. 2019.

[7] H. H. B. Sørensen and P. C. Hansen, "Multicore performance of block algebraic iterative reconstruction methods," *SIAM J. Sci. Comput.*, vol. 36, no. 5, pp. 524–546, 2014.

[8] C. Habermehl, J. Steinbrink, S. Haufe, and K.-R. Müller, "Optimizing the regularization for image reconstruction of cerebral diffuse optical tomography," *J. Biomed. Opt.*, vol. 19, no. 9, Nov. 2014, Art. no. 096006.

[9] Y. LeCun, Y. Bengio, and G. Hinton, "Deep learning," *Nature*, vol. 521, pp. 436–444, May 2015.

[10] Q. Zhang, L. T. Yang, Z. Chen, and P. Li, "A survey on deep learning for big data," *Inf. Fusion*, vol. 42, pp. 146–157, Nov. 2017.

[11] Y. Gao, K. Wang, Y. An, S. Jiang, H. Meng, and J. Tian, "Nonmodel-based bioluminescence tomography using a machine-learning reconstruction strategy," *Optica*, vol. 5, no. 11, pp. 1451–1454, 2018.

[12] J. Feng, Q. Sun, Z. Li, Z. Sun, and K. Jia, "Back-propagation neural network-based reconstruction algorithm for diffuse optical tomography," *J. Biomed. Opt.*, vol. 24, no. 5, 2018, Art. no. 051407.

[13] H. Yin, X. Jiao, Y. Chai, and B. Fang, "Scene classification based on single-layer SAE and SVM," *Expert Syst. Appl.*, vol. 42, no. 7, pp. 3368–3380, May 2015.
[14] M. Xiao, Y. Jiang, Q. Zhu, S. You, J. Li, H. Wang, X. Lai, J. Zhang, and H. Liu, "Diffuse optical tomography of breast carcinoma: Can tumor total hemoglobin concentration be considered as a new promising prognostic parameter of breast carcinoma?" *Acad. Radiol.*, vol. 22, no. 4, pp. 439–446, Apr. 2015.
[15] W. Cong, X. Intes, and G. Wang, "Optical tomographic imaging for breast cancer detection," *J. Biomed. Opt.*, vol. 22, no. 9, Sep. 2017, Art. no. 096011.
[16] H.-I. Suk, S. W. Lee, D. Shen, and Alzheimer's Disease Neuroimaging Initiative, "Latent feature representation with stacked auto-encoder for AD/MCI diagnosis," *Brain Struct. Function*, vol. 220, no. 2, pp. 841–859, Mar. 2015.
[17] R. Jiao, X. Huang, X. Ma, L. Han, and W. Tian, "A model combining stacked auto encoder and back propagation algorithm for short-term wind power forecasting," *IEEE Access.*, vol. 6, pp. 17851–17858, Mar. 2018.

HUIQUAN WANG was born in 1985. He received the bachelor's and Ph.D. degrees in biomedical engineering from the School of Precision Instruments and Optoelectronics Engineering, Tianjin University, the bachelor's degree in international finance from Nankai University, and the Ph.D. degree in instrument science and technology from Tianjin University.

From 2011 to 2013, he was a Public Visiting Scholars study with Johns Hopkins University. He is currently the Director of the Department of Biomedical Engineering and the Master Instructor of Tianjin Polytechnic University. His main research interests include wearable medical testing equipment and intervention methods, near-infrared spectroscopy and big data mining algorithms, multi-modal imaging technology, and so on.

NIAN WU was born in 1994. She received the bachelor's degree in biomedical engineering from the School of Electronics and Information Engineering, Tianjin Polytechnic University, where she is currently pursuing the master's degree in biomedical engineering with the School of Life Sciences.

Her research interests include near-infrared spectroscopy and wearable medical testing equipment.

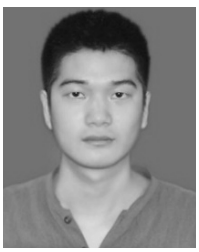

YU CAI was born in 1993. He received the bachelor's degree in electronic information engineering from Shangqiu Teachers College, in 2017. He is currently pursuing the master's degree in biomedical engineering with the School of Life Sciences, Tianjin Polytechnic University.

His research interests include embedded system development and design, and research and development of wearable medical testing equipment.

LINA REN was born in 1993. She received the bachelor's degree in biomedical engineering from the School of Electronics and Information Engineering, Tianjin Polytechnic University, in 2016, and the master's degree in biomedical engineering from the School of Life Sciences, Tianjin Polytechnic University, in 2019.

Her research interests include near-infrared spectroscopy and wearable medical testing equipment.

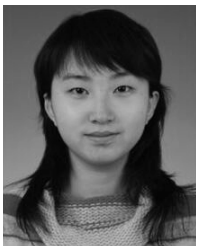

ZHE ZHAO received the bachelor's, master's and Ph.D. degrees in biomedical engineering from the School of Precision Instruments and Optoelectronics Engineering, Tianjin University.

In 2012, she was a National Scholar with the BME Department, Johns Hopkins University, for a one-year visit. She was a Lecturer with Tianjin Polytechnic University, focusing on hyperspectral analysis and complex solution composition analysis.

GUANG HAN received the bachelor's and Ph.D. degrees in biomedical engineering from the School of Precision Instruments and Optoelectronics Engineering, Tianjin University.

He is currently a master's tutor with Tianjin Polytechnic University. His main research interests include noninvasive detection of near-infrared human blood glucose concentration (tissue optics, spectral analysis, chemometrics, optical design, error analysis, etc.), digital image processing (image segmentation, features extraction and identification, etc.), and mechanical design (AutoCAD and Solidworks, etc.).

JINHAI WANG was born in 1966. He received the bachelor's degree from Xi'an Jiaotong University, the master's degree from Tianjin Textile Institute, and the Ph.D. degree from Tianjin University.

He is currently a Professor and a Master Instructor with Tianjin Polytechnic University, and his laboratory is the Tianjin Key Laboratory of Optoelectronic Detection Technology and Systems. He has published more than 100 papers. His research interests include embedded system development and application, information detection and intelligent processing, medical electronic diagnosis and treatment technology and instruments, and modern sensing technology and systems.